CHARACTERIZATION OF THE YARN TENSION EVOLUTION GENERATED BY BRAIDING CARRIERS

C. S. Talos[1,2], S. Achiche[2], L. Laberge Lebel[1,*]

1 : Advanced Composites and Fibres Structures Laboratory, Centre de recherche sur les systèmes polymères et composites à haute performance, Polytechnique Montréal, 2900 boul. Édouard-Montpetit, 2500 ch. de Polytechnique, Montréal, QC H3T 1J4 Canada

2 : Laboratoire de Conception de Systèmes Intelligents et Mécatroniques (CoSIM), Polytechnique Montréal, 2900 boul. Édouard-Montpetit, 2500 ch. de Polytechnique, Montréal, Qc, Canada, H3T 1J4

* Corresponding author (LLL@polymtl.ca)

Keywords: *Braiding, Carrier, Yarn Tension*

ABSTRACT

During the braiding process of composite materials, yarn bobbins are transported by carriers following predefined patterns. The yarns unwind from the bobbins and rub against a series of surfaces such as rollers, curved planes, eyelets, and pulleys that form a tensioning mechanism. This tensioning mechanism provides a root mean squared (RMS) constant tension in the yarn during the process. However, the tensioning system induces impacts on the yarns. The impacts, combined with the friction on the surfaces, cause a deterioration of the mechanical properties of the braids. The objective of this study is to characterize various industry-grade carriers that are used to manufacture braids on a circular braiding machine. An experimental setup using a speed-controlled motor and a custom-made tension measurement device was used. Characterization experiments were done varying the yarn material (glass or nylon), the unwinding speed (between 25 and 250 mm/s), and the stiffness of the springs in the tensioning mechanism. The curve representing the tension with respect to time was observed to have a sawtooth shape with large instantaneous variations. This characterization can help one determine the most desired behavior of the tensioning system for a specific material. This will lead to improved designs for future industry-grade carriers.

1 INTRODUCTION

Braiding of yarns to form a textile structure has been used for many years, with statues dating several years B.C. showing braided hairstyles. The braiding process differs from other textile manufacturing processes such as weaving and knitting since the yarns making the fabric are placed on bobbins in motion. Figure 1a) shows a maypole braiding machine having height bobbin carriers distributed on the braider circumference. Four bobbins, having orange yarns, rotate clockwise and the remaining four, with green yarns, rotate counterclockwise. The carrier motions are guided by a track in the braider bedplate. The carriers follow a path that creates yarn crossovers due to their intertwining motion. The braided structure is pulled away from the moving bobbins plane, generating an elongated structure comprised of yarn crossovers. The first noticeable introduction of braiding to the aeronautics field was led by NASA for the "Automated Composite Technology" (ACT) program in 1997 [1]. Braids of reinforcing fibers, such as glass or carbon, were incorporated into polymer resin by Liquide Composite Molding (LCM) processes to get the final part.

The braiding of composite materials allows, after consolidation, the manufacturing of stiff, strong and lightweight structures. Recently, this process has been successfully demonstrated for the manufacturing of aircraft fuselage frames [2-5]. Also, braids of hybrid carbon and thermoplastic polymer yarns can be pultruded to form a thermoplastic beam reinforced by a carbon fiber braid structure [6-8].

Figure 1b-c) shows typical yarn carriers used with braiding machines. A bobbin onto which the yarn is wound is installed on the bobbin shaft. The yarn passes onto friction surfaces and pulleys to guide it in the spring activated tension control dancer arm. In carriers, the bobbin rotation is blocked by a pawl that is released with the action of the dancer arm.

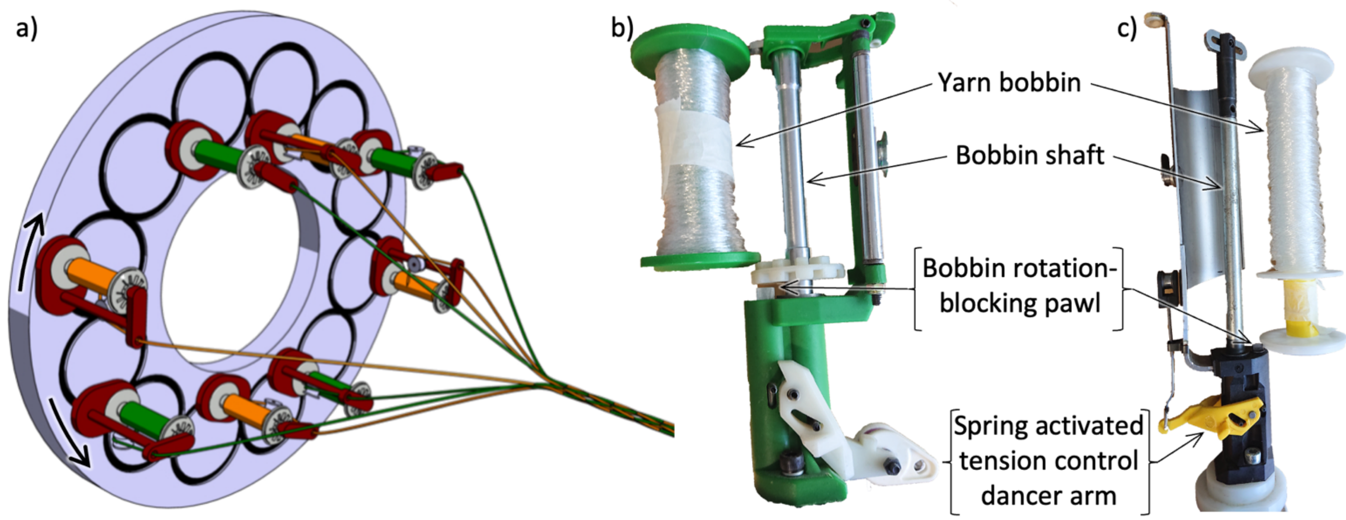

Figure 1. a) Representation of a braiding machine with 4 carriers with orange yarns rotating clockwise and 4 carriers with green yarns rotating counterclockwise. b) db.SFCA carrier. c) db.CTT carrier.

Figure 2 shows a detailed view of the tension control mechanism of braiding carriers. The yarn unwinds from the carriers by passing through multiple pulleys and friction-inducing surfaces. The yarn is guided to pass onto the dancer arm pulley and is then pulled through the carrier yarn-feeding eyelid towards the braid. Figure 2a),d) show the situation when the dancer arm is at its lowest position. The pawl is engaged in the bobbin and therefore stopping the bobbin rotation. Figure 2b),e) show the yarn being pulled from the carrier, raising the dancer arm towards the yarn-feeding eyelid. The pawl is still engaged in the bobbin to block its rotation. The dancer arm's raise is counteracted by two springs. A low-stiffness spring located in the bobbin shaft (in blue in Figure 2) is compressed first. Once the dancer arm reaches its highest point, it moves the pawl away from the bobbin. The pawl movement is counteracted by a second stiffer spring. Figure 2c),f) show the state when the dancer arm action has removed the pawl from the bobbin. At this point, the bobbin is free to rotate. The unwinding of the yarn then lowers the dancer arm therefore re-engaging the pawl into the bobbin to block its rotation. The spring activated dancer arm creates an oscillatory tension in the yarn due to the springs' reaction force variation. While the average yarn tension force is adjusted by replacing the main spring, the oscillatory nature of the tension force cannot be changed due to the carrier architecture. Zhang *et al.* have observed that these tension variations can induce damage in carbon fibers during braiding [9]. Few studies thoroughly characterize the oscillatory nature of the tension in yarn carriers for braiding. The objective of this study is to characterize the effects of the carrier architecture, the spring stiffness, the yarn unwinding speed, and the type of yarn material on the yarn tension during unwinding.

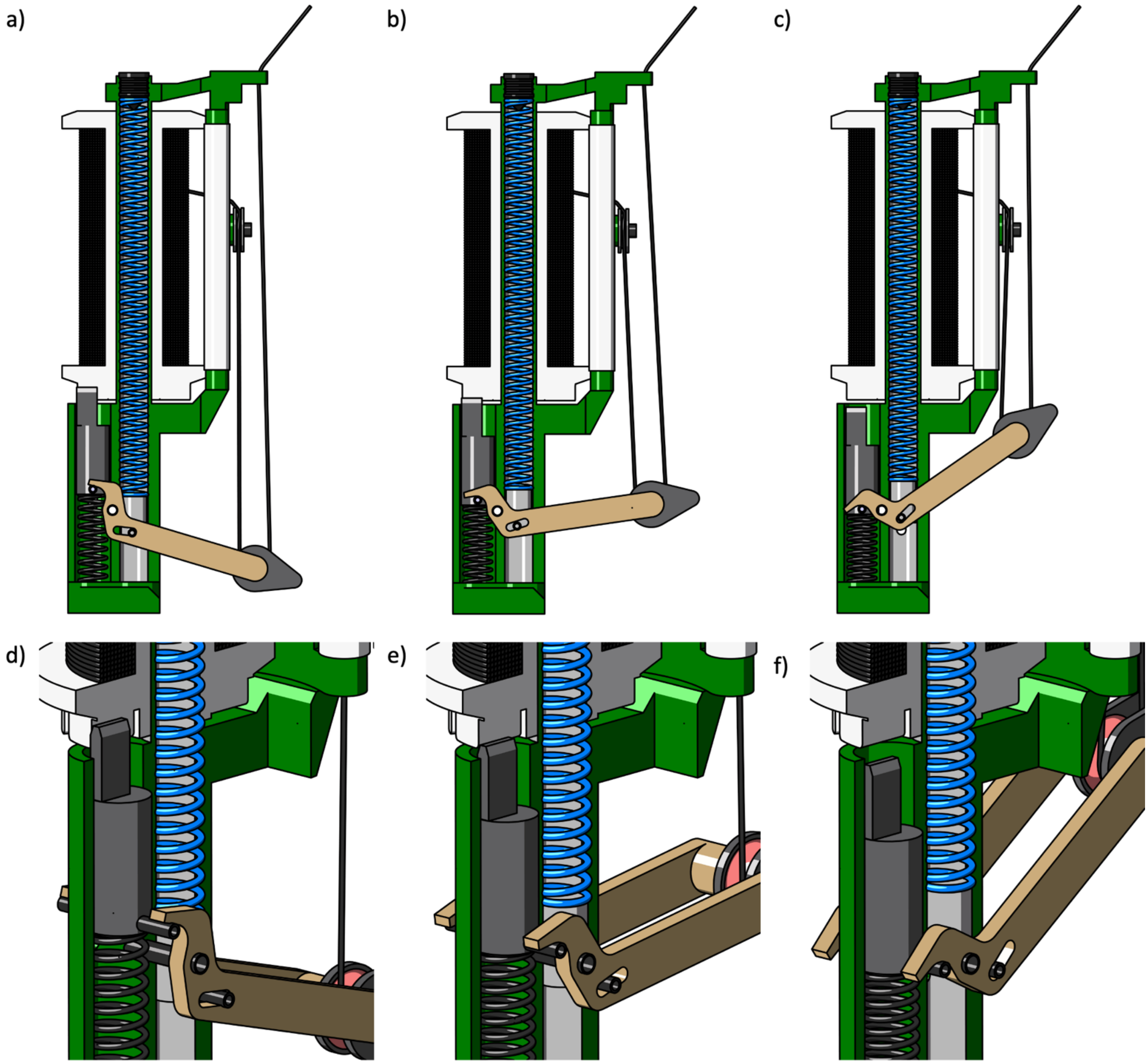

Figure 2. Steps of the tension regulation system in braiding carriers: a),d) The pawl is engaged in to block the bobbin rotation; b),e) the pulling of the yarn from the carrier elevates the dancer arm, therefore lowering the pawl; c),f) when the dancer arm is at the top of its range, the pawl is pulled out, therefore liberating the bobbin rotation. The blue spring encased in the bobbin shaft is the tension control spring that can be changed to vary yarn tension.

2 EXPERIMENTAL

Figure 3 shows the yarn tension measurement apparatus developed for this study. The carriers were attached to the wooden base of the apparatus (Figure 3-1). The yarns were taken from the carrier yarn-feeding eyelid and passed through a yarn tension sensor (Figure 3-2). This sensor was composed of three pulleys, with the middle one being fixed onto a loadcell. The yarn zigzagged over-under-over the three pulleys. The yarn tension exerted a resultant force on the middle pulley which was measured by the loadcell. The yarn was then wound onto a pickup bobbin actioned by a brushless direct current motor (Figure 3-3). The motor is controlled by a drive (ODrive Robotics, Figure 3-7) connected to a Raspberry Pi computer (Figure 3-8). This computer also registered the tension data from the tension sensor through an analog to digital converter (Figure 3-6). The data acquisition rate was set at 7500 Hz.

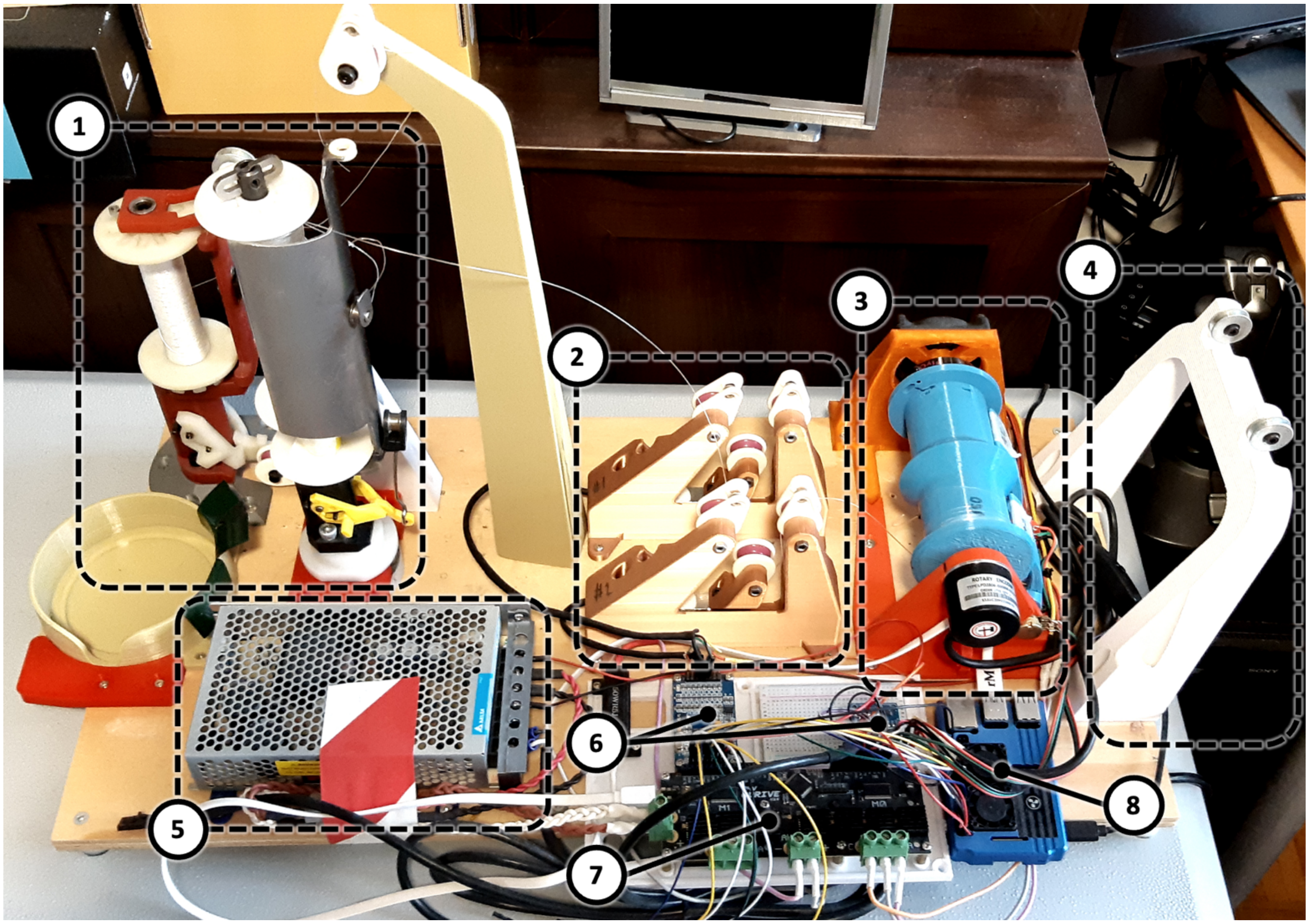

Figure 3. Tension measurement apparatus used to characterize yarn tension: 1-Carriers, 2-Yarn Tension Sensor, 3-Winding station, 4-Calibration pulleys, 5-Power Supply, 6-Digital to Analog Converters, 7-Motor Drive, 8-Raspberry PI computer.

Table 1 lists the tested parameters. Two carrier architectures were tested. The db.SFCA was the A03 model from Xuzhou Henghui Braiding Machine Co. Ltd. The db.CTT was the IFDA100 model from Herzog Gmbh. The db.SFCA was tested with five different springs having nominal stiffness of 7, 19, 39, 83 and 369 N/m. The db.CTT was tested with four different springs having stiffness of 29, 81, 130, and 426 N/m. In the table, the carrier/spring combination is indicated by the letters identifying the carrier and the spring stiffness. Five unwinding speeds were selected, from 25 mm/s to 250 mm/s. Finally, two types of yarns were tested. The first yarn is a nylon fishing line; a monofilament yarn with a diameter of 60 µm. The second yarn was a glass multifilament yarn (EC7 22 1X0 Z40 620-1, AGY). The yarn size was 22 tex. It was composed of 204 glass filaments of approximately 7 µm in diameter. The glass fibers had a starch-based sizing (620-1) for lubrication purposes. The yarn was twisted at 40 turns per meters. A full factorial experimental design of experiments was carried out, for a total of $9^1 5^1 2^1 = 90$ conditions. Each condition was repeated 3 times. The test was done for 15 seconds of unwinding. Only the last 10 seconds at steady state conditions were analyzed. The raw data was filtered with a median filter on 201 values. The raw data was also treated with a Fast Fourier Transform to determine the component frequencies in the tension signal.

Table 1. Conditions for tension measurement experiments.

Carrier-Spring Configuration	Unwinding speed (mm/s)	Yarn Type
SFCA-7	25	Nylon Monofilament
SFCA-19	50	Glass Fiber
SFCA-39	100	
SFCA-83	150	
SFCA-369	250	
CTT-59		
CTT-81		
CTT-130		
CTT-425		

3 RESULTS AND DISCUSSION

Figure 4 presents the tension measured during the 15-second test of the db.CTT carrier (Figure 1b), unwinding at 25 mm/s, with the glass fiber yarn. The photos presented in Figure 4a-e) show the position of the dancer arm at different stages of the tension curve. Figure 4f) shows the evolution of the tension during the unwinding. The Noisy curve is the raw data. The Noisy curve consists of the 112,500 data points acquired by the tension measurement apparatus. The Filtered curve is obtained after applying the median filter on the raw data. At point a), the dancer arm was at its lowest point since there was no tension in the yarn. The tension gradually increased until reaching a plateau where the dancer arm is at an intermediary position (Figure 4b). The tension plateau can be attributed to the shape of the connection between the dancer arm and the tension spring, as well as slacks being retaken in the yarn. Then, the dancer arm was raised to its high point (Figure 4c) where the pawl was disengaged from the bobbin. Before disengaging, the tension in the yarn was at a maximum value of 4.1 N. After disengaging, the dancer arm rapidly lowered due to the bobbin rotation unwinding the yarn. At Figure 4d) the dancer arm stopped at its lowest point when the pawl re-engaged in the bobbin to stop its rotation. This dancer arm position corresponds to a minimum tension of 2.4 N (point “d” on Figure 4f). The up and down movement was repeated with yarn pulling creating a sawtooth shape on the tension vs unwinding time chart. The tension oscillated from approximately 2.4 N to 4.1 N. The frequency of this oscillation was approximately 1.125 Hz. The yarn tension drop from its maximum to its minimum was rather sharp. The drop occurred on the duration of approximately 0.1 s. The raw data and the filtering data also seem to indicate a rebound phenomenon at the minimum tension value, since the tension curve minimum is not sharply defined. The sharp drop and rebound are likely to create damage on stiff but fragile fiber materials such as glass and carbon. A video of the tested condition of Figure 4, along with other tested conditions can be seen at https://youtu.be/rbnXGFDRUkI.

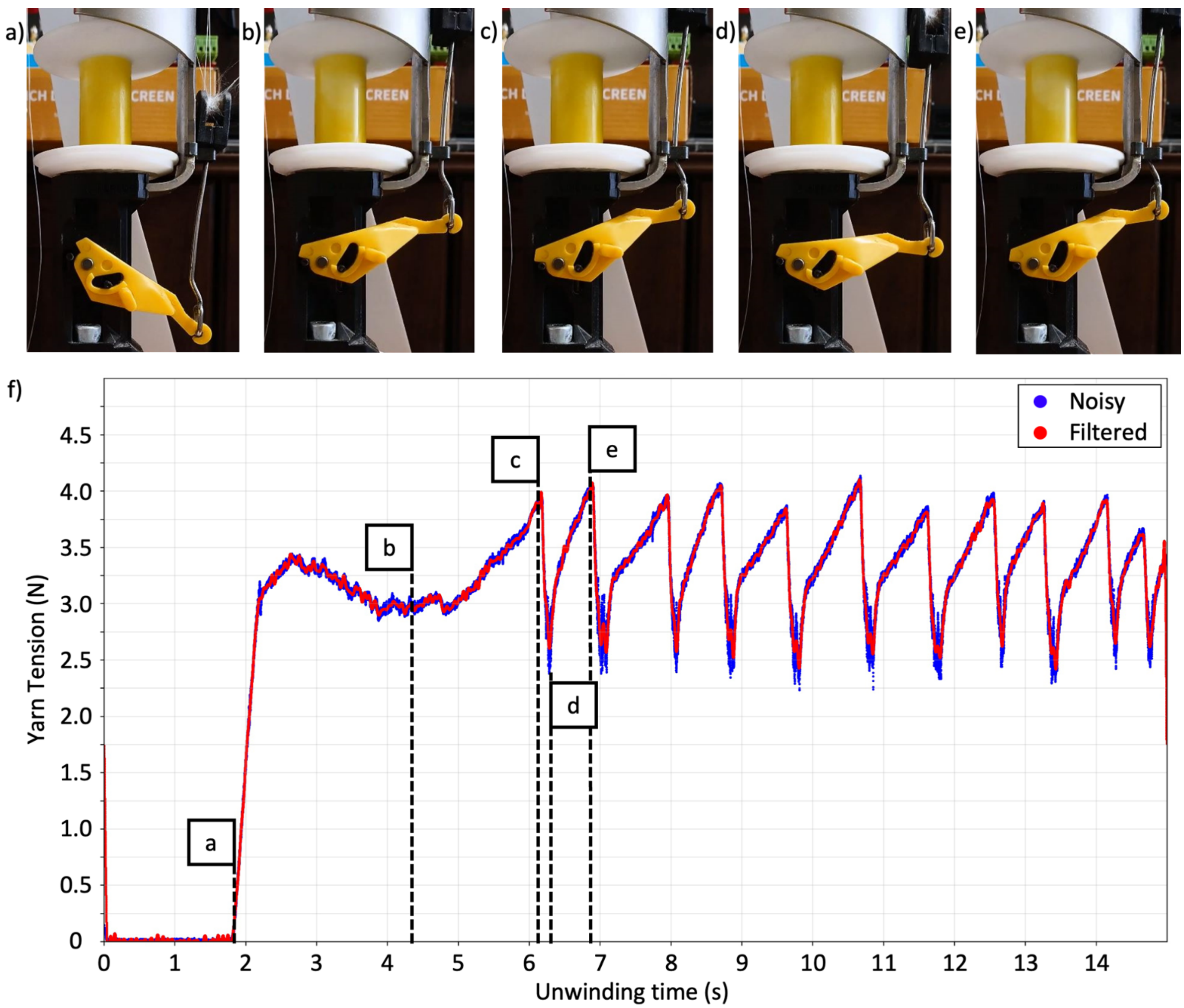

Figure 4. Yarn Tension at unwinding speed of 25 mm/s for the db.CTT with a glass fiber yarn and the 435 N/m spring. a) The yarn starts the pulling of the dancer arm. b) Transitory tension regime. c) Maximum yarn tension at the dancer arm high point. d) Low tension point when the dancer arm is at is low point after bobbin unwinding. e) Repeated high tension with the dancer arm at high position.

Figure 5 presents the typical data analysis done for each tested condition. This particular test was the db.SFCA carrier, with the 39 N/m spring, unwinding at 100 mm/s. In Figure 5a) the raw and filtered tension variation is presented with respect to the unwinding time. The first five seconds of the data was discarded to reach steady-state conditions. The filtered data from 5 seconds to 15 seconds was analyzed. In this situation, the average tension was 0.59 N $\pm$ 0.08. The minimum tension registered was 0.26 N, the highest tension 0.81 N. Figure 5b) presents a histogram of the tension data points. The highest number of individual tension measurements was registered at approximately 0.6 N, in accordance with the tension average of 0.59 N. The distribution seems to be normal with equal amounts of data below and above the average for both the filtered (dark green) and the raw data (light green).

This situation was quite exceptional since few conditions had a normal distribution of tension data points. Notwithstanding this fact, it was decided to keep a standard deviation to characterize the range of tensions from each tested condition. From Figure 5c) it is seen that the dominant frequencies are under 40 Hertz. The highest peak is between 0 and 5 hertz, corresponding to the main tension variations of the yarn tension vs unwinding time chart of Figure 5a). Other peaks are seen at higher frequencies. However, they could not be assigned to physical phenomena. This will be done in future work.

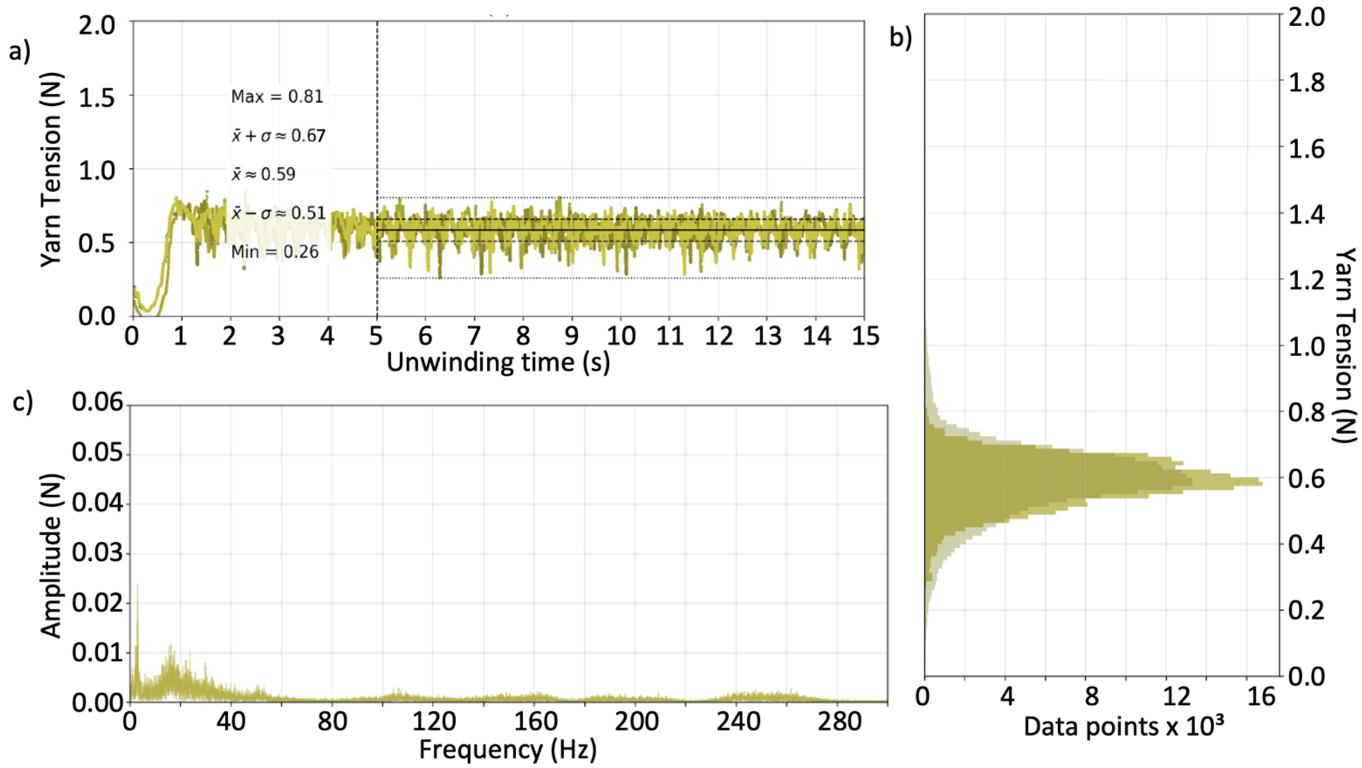

Figure 5. a) Raw (light green) and filtered (dark green) tension data of the db.SFCA carrier, with the 39 N/m spring, unwinding at 100 mm/s. The vertical dashed line is the start of the steady-state evaluation, the horizontal line is the tension average, the dashed lines are one standard deviation, the dotted lines are max and min values of the tension. b) histogram of tension. c) Spectral analysis on the filtered data between 5 s and 15 s.

Figure 6 shows the tension averages for all tested unwinding speeds, carriers, springs nominal stiffness and material type. For the db.SFCA, tension averages varied between 0.29 N and 1.41 N. For the db.CTT, tension averages varied between 0.72 N and 3.84 N. The main factor influencing the tension average was the nominal spring stiffness for a given carrier. No effect of the material type (nylon or glass fiber), nor the unwinding speed was observed since the fluctuations of the averages all fall within the standard deviations. The standard deviations varied within the [0.05,0.21] N interval for the db.SFCA. The standard deviations varied within the [0.06,0.56] N interval for the db.CTT. The standard deviations were generally larger for the higher stiffness springs. This was expected since the tension variations at higher spring stiffness were larger due to larger load levels needed to liberate the rotation of the bobbin. As for the tension averages, the material type and unwinding speed did not seem to influence the standard deviations. It is not clear whether if the carrier type influenced the standard deviations since they seemed to be comparable for equivalent tension averages.

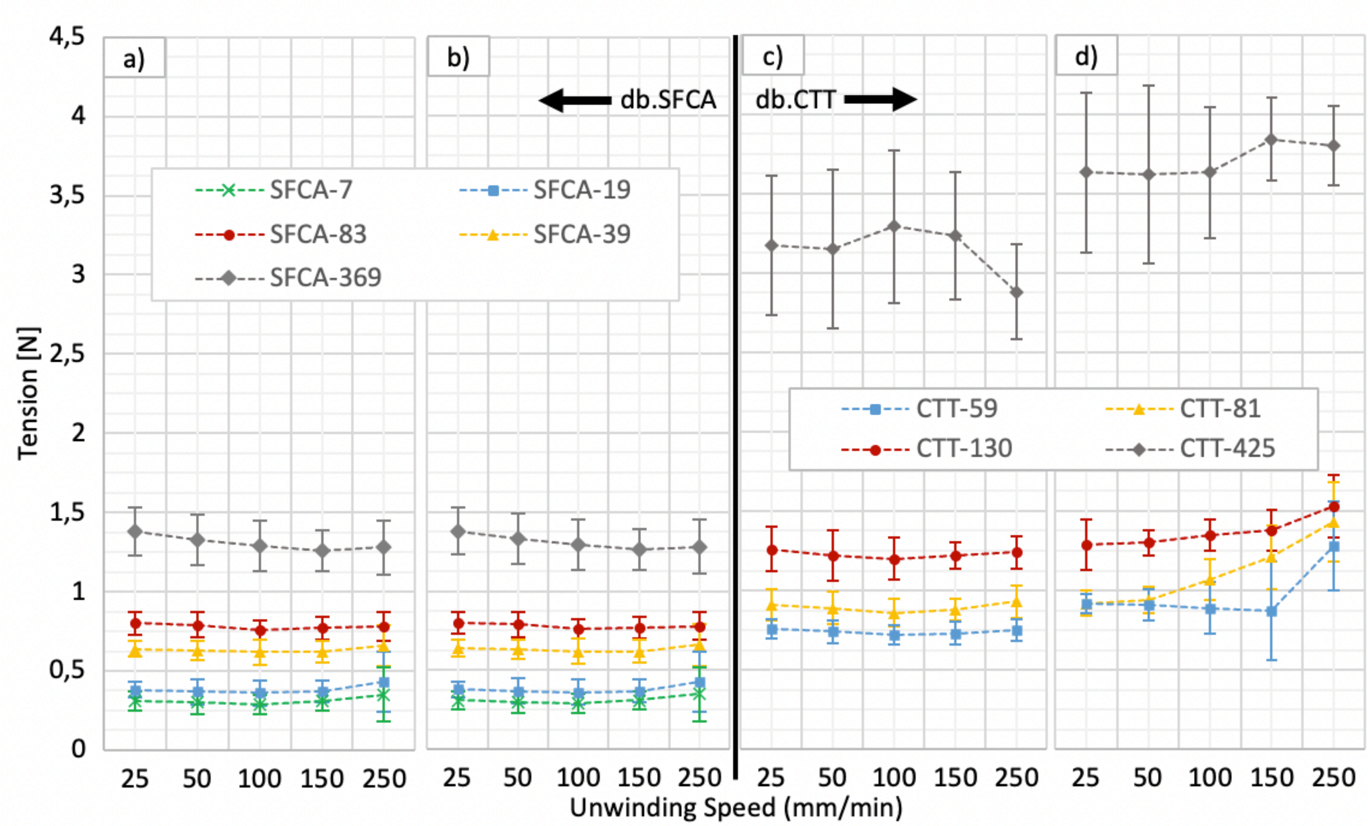

Figure 6. Tension averages at tested speeds in steady state conditions for the different springs. Error bars are one standard deviation. a) db.SFCA with nylon yarn. b) db.SFCA with glass fiber yarn. c) db.CTT with nylon yarn. d) db.CTT with glass fiber yarn.

4 CONCLUSIONS

The objective of this study was to characterize the tension behavior of yarns fed by two different carrier types used in composite manufacturing. The effect of carrier architecture, yarn material, unwinding speed, and spring stiffness were investigated by performing a full factorial experimental design of 90 conditions. Each condition was repeated 3 times. It was found that the tension has a sawtooth behavior with unwinding length due to the carrier architecture. The carriers regulated the tension through a spring-reacted dancer arm. When the dancer arm reached its uppermost position, it released the bobbin rotation that was feeding yarn and generating a rapid drop in tension until it blocked sharply. This sharp tension peek could be responsible for the yarn damage. The average tension was between 0.29 N and 1.41 N for the db.SFCA, and between 0.72 N and 3.84 N for the db.CTT. The average tension was influenced by the main spring into the carrier. The standard deviation on tension for every individual condition was in the 0.05 N to 0.56 N. No effect of the carrier architecture, the material type and unwinding speed could be observed. The main clear reason for increasing averages and standard deviations was the spring stiffness that increased between tested conditions. This research work will support designers through guidelines to create new carrier architectures without tension variations. In future studies, the parameters characterized will be reproduced in a fully automated braiding carrier where the tension can be adjusted remotely and instantaneously.

5 ACKNOLEGEMENTS

The authors would like to thank the financial support of FilSpec inc., Bauer Hockey Ltd., Pultrusion Technique, the Natural Sciences and Engineering Research Council (NSERC, CRDPJ 543847-19) and Quebec's Advanced Materials Research and Innovation Hub (PRIMA Québec, R18-13-003).

6 REFERENCES

1. Dow, M.D. and H.B. Dexter. "Development of stitched, braided and woven composite structures in the ACT program and at Langley Research Center". NASA/TP-97-206234, National Aeronautics and Space Administration, Hampton, Virginia, Unites States, 1997.
2. Gardiner, G. "Airbus A350 Update: BRaF & FPP". CompositeWorld, 2012.
3. Gondran, M., Y. Abdin, Y. Gendreau, F. Khameneifar, and L. Laberge Lebel. "Automated braiding of non-axisymmetric structures using an iterative inverse solution with angle control". *Composites Part A: Applied Science and Manufacturing*, Vol. 143, No., pp., 2021.
4. Laberge Lebel, L. and P. Trudeau. "Preforming of a Fuselage C-Shaped Frame Manufactured by Resin Transfer Molding". *SAE International Journal of Aerospace*, Vol. 6, No. 2, pp. 508-512, 2013.
5. Monnot, P., J. Lévesque, and L. Laberge Lebel. "Automated braiding of a complex aircraft fuselage frame using a non-circular braiding model". *Composites Part A: Applied Science and Manufacturing*, Vol. 102, No., pp. 48-63, 2017.
6. Ghaedsharaf, M., J.-E. Brunel, and L. Laberge Lebel. "Multiscale numerical simulation of the forming process of biaxial braids during thermoplastic braid-trusion: Predicting 3D and internal geometry and fiber orientation distribution". *Composites Part A: Applied Science and Manufacturing*, Vol. 150, No., pp., 2021.
7. Ghaedsharaf, M., J.E. Brunel, and L. Laberge Lebel. "*Thermoplastic composite rod manufacturing using biaxial braid-trusion"*. in *18th European Conference on Composite Materials, ECCM 2018, June 24, 2018 - June 28, 2018*. Athens, Greece: Applied Mechanics Laboratory. pp. Adamant Composites Ltd.; Hellenic Aerospace Industry S.A; JEC Group; Materials Today; Photron; Shimadzu Europa GmbH, Document Number, 2020.
8. Lebel, L.L. and A. Nakai. "Design and manufacturing of an L-shaped thermoplastic composite beam by braid-trusion". *Composites Part A: Applied Science and Manufacturing*, Vol. 43, No. 10, pp. 1717-29, 2012.
9. Zhang, Y., Z. Meng, L. Su, and Y. Sun. "Modeling and analysis of carbon fiber carrier tension systems used in 3D braiding machine". *Journal of Engineered Fibers and Fabrics*, Vol. 14, No., pp., 2019.